

Vacuum Brazing TC4 Titanium Alloy to 304 Stainless Steel with Cu-Ti-Ni-Zr-V Amorphous Alloy Foil

Honggang Dong, Zhonglin Yang, Zengrui Wang, Dewei Deng, and Chuang Dong

(Submitted March 19, 2014; in revised form June 18, 2014; published online July 17, 2014)

Dissimilar metal vacuum brazing between TC4 titanium alloy and 304 stainless steel was conducted with newly designed Cu-Ti-Ni-Zr-V amorphous alloy foils as filler metals. Solid joints were obtained due to excellent compatibility between the filler metal and stainless steel substrate. Partial dissolution of stainless steel substrate occurred during brazing. The shear strength of the joint brazed with $\text{Cu}_{43.75}\text{Ti}_{37.5}\text{Ni}_{6.25}\text{Zr}_{6.25}\text{V}_{6.25}$ foil was 105 MPa and that with $\text{Cu}_{37.5}\text{Ti}_{25}\text{Ni}_{12.5}\text{Zr}_{12.5}\text{V}_{12.5}$ was 116 MPa. All the joints fractured through the gray layer in the brazed seam, revealing brittle fracture features. Cr_4Ti , $\text{Cu}_{0.8}\text{FeTi}$, Fe_8TiZr_3 and $\text{Al}_2\text{NiTi}_3\text{C}$ compounds were found in the fractured joint brazed with $\text{Cu}_{43.75}\text{Ti}_{37.5}\text{Ni}_{6.25}\text{Zr}_{6.25}\text{V}_{6.25}$ foil, and Fe_2Ti , TiCu , Fe_8TiZr_3 and $\text{NiTi}_{0.8}\text{Zr}_{0.3}$ compounds were detected in the joint brazed with $\text{Cu}_{37.5}\text{Ti}_{25}\text{Ni}_{12.5}\text{Zr}_{12.5}\text{V}_{12.5}$ foil. The existence of Cr-Ti, Fe-Ti, Cu-Fe-Ti, and Fe-Ti-V intermetallic compounds in the brazed seam caused fracture of the resultant joints.

Keywords 304 stainless steel, amorphous foil, microstructure, shear strength, Ti-6Al-4V titanium alloy, vacuum brazing

1. Introduction

TC4 titanium alloy (Ti-6Al-4V), with high specific strength and excellent corrosion resistance, is widely used as structural material in aerospace with the purpose of weight reduction and as corrosion-resistant material in non-aerospace industries (Ref 1, 2). However, the high cost due to the complicated smelting process of titanium alloys restricts their extensive applications. However, type 304 stainless steel (304SS) with excellent corrosion resistance and comprehensive performance is one of the most widely used stainless steel, and its price is relatively low. Therefore, dissimilar metal joint between TC4 titanium alloy and 304SS provides an effective approach to combine advantages of both materials.

It is well known that fusion welding has difficulty in joining titanium to steel due to the massive generation of Fe-Ti intermetallic compounds and high-level residual stress produced during welding (Ref 3). However, for solid-state welding and brazing processes, the parent metal does not melt and the formation of intermetallic compounds could be controlled. So, the welding between titanium alloy and steel concentrated in friction welding (Ref 4-8), diffusion welding (Ref 9-14), and brazing (Ref 15-19). Compared to friction welding and diffusion welding, brazing process possesses advantages in

joint design, residual stress reduction, and controlling the generation of brittle Ti-Fe intermetallic compounds.

Liu et al. (Ref 15) brazed Ti-6Al-4V alloy to 304SS with three commercially available Ag-based fillers and found that both BAG-8/304SS and Ticusil/304SS interfaces contained thick Cu-Ti-Fe reaction layer which reduced the wettability of BAG-8 and Ticusil fillers on the 304SS substrate. Shiue et al. (Ref 16, 17) studied the effect of Ni and (Ni)-Cr barrier layers on brazing Ti-6Al-4V alloy to 17-4 PH stainless steel with Ag-based fillers, and concluded Ni and (Ni)-Cr barrier layers were effective in avoiding Fe-Ti intermetallic compounds. The largest average shear strength of Ti-6Al-4V alloy/17-4 PH stainless steel joints was 243 MPa due to the replacement of Fe-Ti intermetallic compounds by Ti-Cu-(Ni) and/or TiCr_2 phases. However, the tensile strength and creep strength of most Ag-based alloys at temperatures above 400 °C are inferior to that of Ti-based fillers (Ref 20); especially, the Ag-based fillers are very expensive and their extensive applications are limited.

Botstein et al. (Ref 21) brazed Ti-6Al-4V alloy using 25Ti-25Zr-50Cu (wt.%) amorphous alloy as filler metal, and solid joints with the same tensile strength level as that of base metal were obtained. Ti-15Cu-25Ni and Ti-15Cu-15Ni (wt.%) alloy foils were used to braze Ti50Al50 and Ti-6Al-4V alloys by Shiue et al. (Ref 20). Both Ti50Al50 and Ti-6Al-4V alloys obviously reacted with the filler metals, though reacted region had different shapes. The largest shear strength was acquired as 280 MPa, and the Ti_2Ni and Ti_3Al phases existing in the brazed seam deteriorated the shear strength of the joint. Ganjeh et al. (Ref 22) investigated the brazing of commercial pure titanium and Ti-6Al-4V alloy with Ti-based (Ti-27Zr-14Cu-13Ni, wt.%) amorphous foil. Strong reaction between the molten filler and Ti-6Al-4V alloy substrate occurred during brazing with optimum average shear strength of 571 MPa. However, brazing titanium to steel with Ti-based filler metal was seldom reported considering the incompatibility between Ti-based filler metal and steel substrate (Ref 23).

For the purpose of improving the affinity between Ti-rich filler metal and steel, new types of amorphous Ti-Cu-based

Honggang Dong, Zhonglin Yang, Zengrui Wang, and Dewei Deng, School of Materials Science and Engineering, Dalian University of Technology, Dalian 116024, People's Republic of China; and Chuang Dong, Key Lab of Materials Modification, Dalian University of Technology, Ministry of Education, Dalian 116024, People's Republic of China. Contact e-mail: donghg@dlut.edu.cn.

filler metals with competitive cost were designed in this paper by reducing Ti content but adding V in the filler. It is well known that Ni and Zr can significantly improve the glass-forming ability of Ti-Cu alloys (Ref 24) and V has infinite solid solubility with both Fe and Ti, so the composition of the filler metal was determined as Cu-Ti-Ni-Zr-V. Then the TC4 titanium alloy and 304 stainless steel were brazed with the developed filler metals, and the microstructure and mechanical properties of the brazed joints were investigated.

2. Experimental Procedures

The base metals to be brazed are TC4 titanium alloy and 304 stainless steel with dimensions of $20 \times 8 \times 2$ mm and $45 \times 20 \times 1.3$ mm, with the chemical composition of Ti-6Al-4V (wt.%) and Fe-0.08C-19Cr-9Ni-2Mn-1Si (wt.%), respectively. The developed Ti-Cu-based amorphous alloys, $\text{Cu}_{43.75}\text{Ti}_{37.5}\text{Ni}_{12.5}\text{Zr}_{12.5}\text{V}_{12.5}$ and $\text{Cu}_{37.5}\text{Ti}_{25}\text{Ni}_{12.5}\text{Zr}_{12.5}\text{V}_{12.5}$ (at.%) with dimensions of 50- μm thick and 2-mm wide, were prepared as filler metals by melt spinning. The XRD patterns in Fig. 1 reveal the amorphous structure of two foils with uniform composition and good flowability in melting state. Differential thermal analysis (DTA) was performed to determine the melting ranges of two filler metals. According to the DTA results, the $\text{Cu}_{43.75}\text{Ti}_{37.5}\text{Ni}_{12.5}\text{Zr}_{12.5}\text{V}_{12.5}$ foil has a melting range from 828 to 849 °C, and the $\text{Cu}_{37.5}\text{Ti}_{25}\text{Ni}_{12.5}\text{Zr}_{12.5}\text{V}_{12.5}$ foil from 859 to 876 °C. Generally, the brazing temperature is 30-90 °C above the liquidus of filler metal (Ref 25), so the brazing temperature in this paper was 900 °C for $\text{Cu}_{43.75}\text{Ti}_{37.5}\text{Ni}_{12.5}\text{Zr}_{12.5}\text{V}_{12.5}$ foil and 930 °C for $\text{Cu}_{37.5}\text{Ti}_{25}\text{Ni}_{12.5}\text{Zr}_{12.5}\text{V}_{12.5}$ foil.

The faying surfaces of the workpieces were polished with SiC papers up to grit 1200 and ultrasonically cleaned in acetone prior to brazing. Then they were assembled into a sandwich as shown in Fig. 2. The filler metal was placed between the workpieces, and a graphite block with gravity of 1kN was

placed upon the assembly to keep the workpieces and filler metal closely contact with each other. The brazing process was conducted in a furnace with a vacuum atmosphere of 4×10^{-3} MPa. The heating rate was set at 10 °C/min throughout the experiment. Before heated up to the brazing temperature, the specimens were preheated at 800 °C for 5 min for temperature homogeneity. Then the assemblies were brazed at 900 or 930 °C for 10 min. For each set of brazing parameters, four couples of specimens were brazed. One was used for the microstructure examination, and the other three were tested to obtain the average shear strength.

The brazed joints were cut by a wire cutting machine, then rubbed with 1200[#] metallographic sandpaper, and finally polished with 0.5- μm diamond paste. Then the cross sections of the joints were observed with Olympus OLS4000 optical microscope, and the elemental distribution in the brazed seam was examined using Shimadzu EPMA-1600 electron probe microanalyzer with 1- μm beam spot at 15 kV. The room temperature shear strength of the joints was evaluated with DNS100 universal tensile machine. Fracture surfaces were observed with JSM-5600LV scanning electron microscope (SEM), and x-ray diffraction (XRD) was conducted with Bruker D8 Focus x-ray diffractometer to determine the phases in the interfaces.

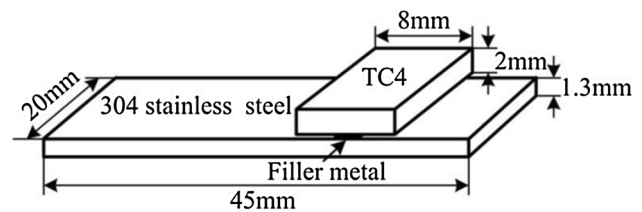


Fig. 2 The schematic diagram of assembling the workpieces and filler metal

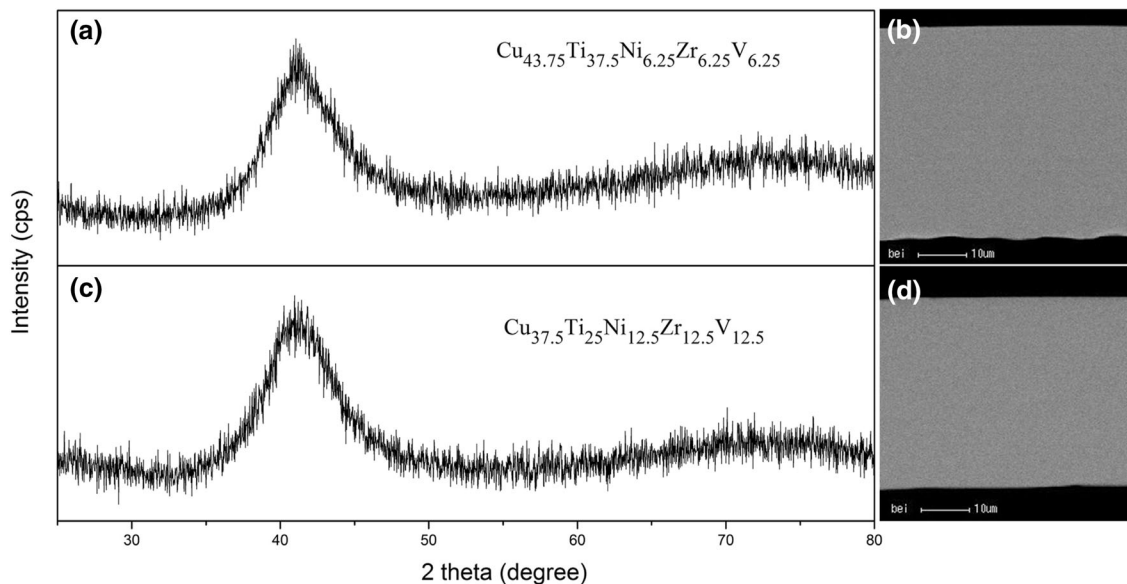


Fig. 1 XRD patterns and backscattered electron images of (a) $\text{Cu}_{43.75}\text{Ti}_{37.5}\text{Ni}_{12.5}\text{Zr}_{12.5}\text{V}_{12.5}$ (at.%) and (b) $\text{Cu}_{37.5}\text{Ti}_{25}\text{Ni}_{12.5}\text{Zr}_{12.5}\text{V}_{12.5}$ (at.%) filler metals

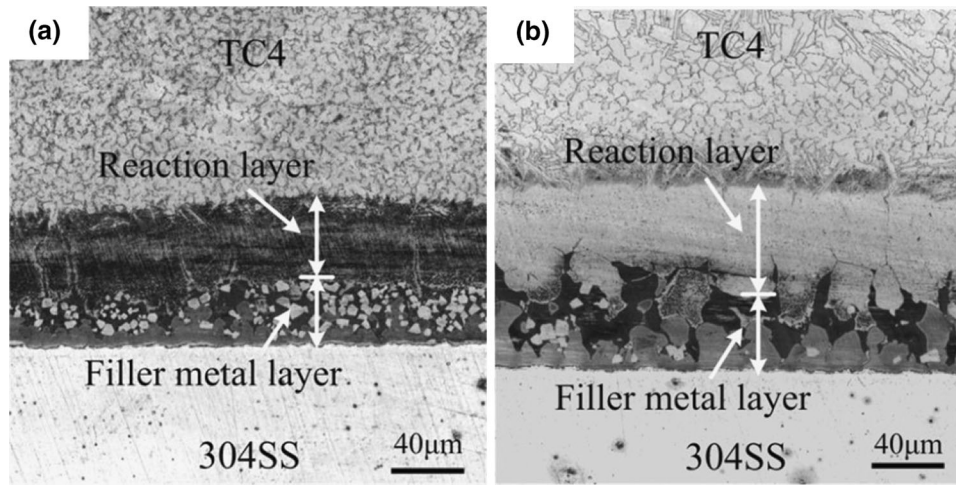


Fig. 3 Microstructure of the joints brazed with (a) $\text{Cu}_{43.75}\text{Ti}_{37.5}\text{Ni}_{6.25}\text{Zr}_{6.25}\text{V}_{6.25}$ foil and (b) $\text{Cu}_{37.5}\text{Ti}_{25}\text{Ni}_{12.5}\text{Zr}_{12.5}\text{V}_{12.5}$ foil

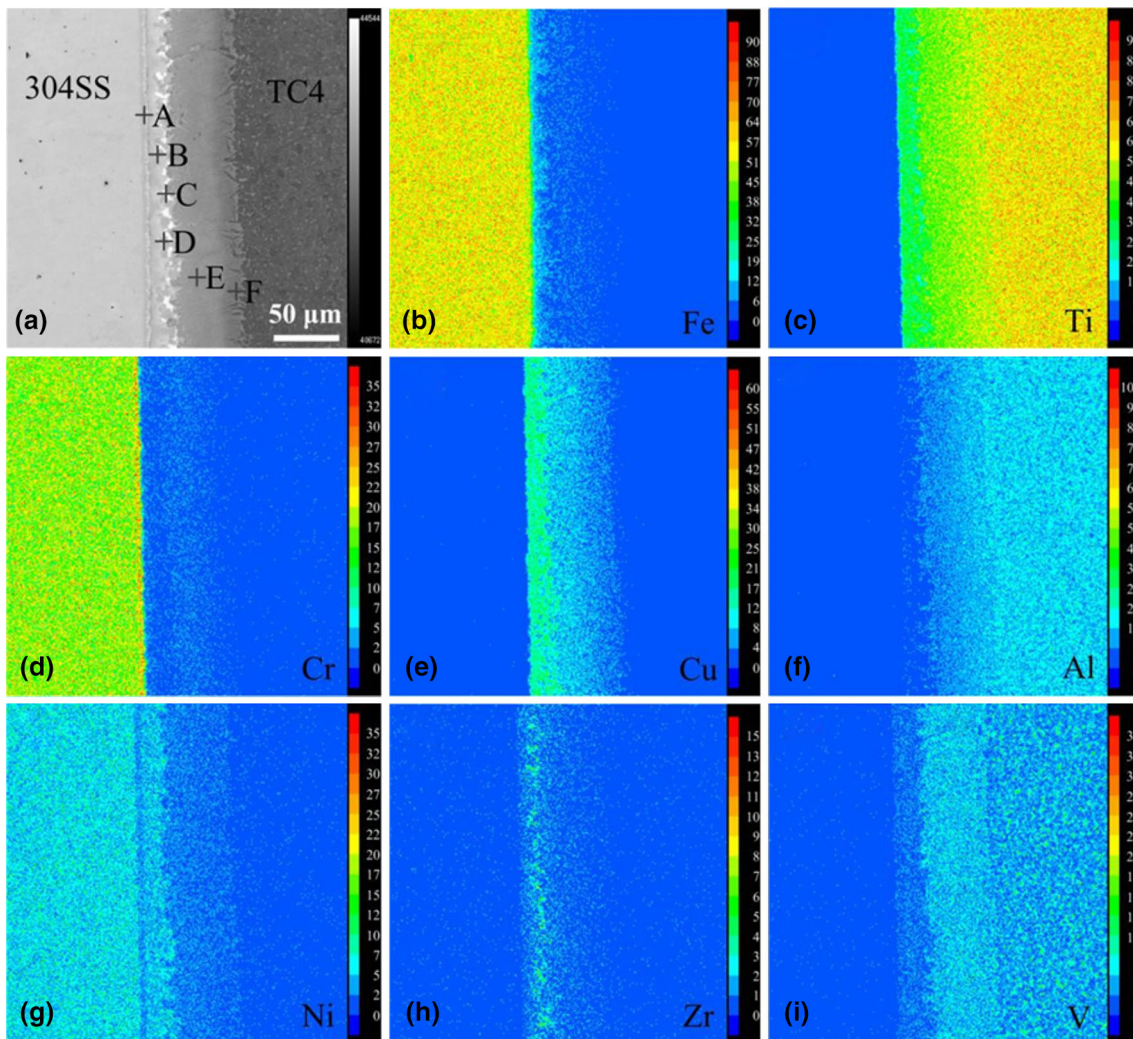


Fig. 4 Backscattered electron image and EPMA map scanning results of the joint brazed $\text{Cu}_{43.75}\text{Ti}_{37.5}\text{Ni}_{6.25}\text{Zr}_{6.25}\text{V}_{6.25}$ (at.%) foil

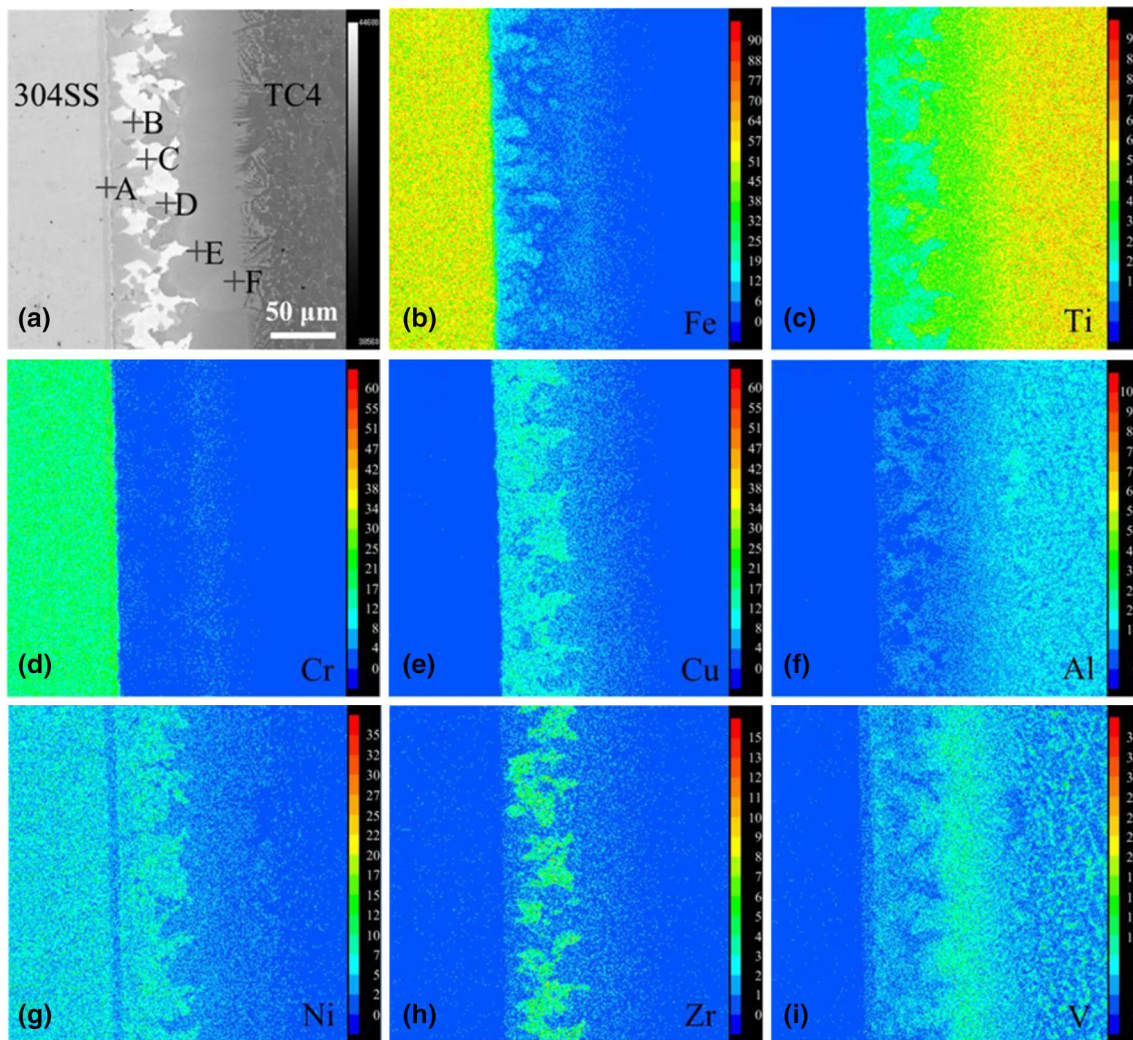


Fig. 5 Backscattered electron image and EPMA map scanning results of the joint brazed $\text{Cu}_{37.5}\text{Ti}_{25}\text{Ni}_{12.5}\text{Zr}_{12.5}\text{V}_{12.5}$ (at.%) foil

Table 1 EPMA quantitative analysis results in locations A-F marked in Fig. 4(a) (at.%)

Location	Fe	Cr	Ti	Al	Cu	Ni	Zr	V
A	66.87	27.46	2.51	0.42	0.65	0.53	0.03	1.53
B	11.24	1.69	50.77	4.43	23.82	4.57	1.36	2.13
C	4.14	0.71	39.69	7.81	30.16	4.28	11.06	2.16
D	7.16	0.77	63.26	1.81	16.78	6.00	1.83	2.40
E	3.77	1.22	67.47	7.57	12.38	1.79	1.89	3.91
F	2.89	0.70	73.34	9.55	6.31	1.07	0.36	5.78

Table 2 EPMA quantitative analysis results in locations A-F marked in Fig. 5(a) (at.%)

Location	Fe	Cr	Ti	Al	Cu	Ni	Zr	V
A	66.77	25.98	2.92	0.52	0.58	1.21	0.00	2.02
B	14.28	2.91	51.48	5.54	14.30	4.91	1.49	5.10
C	8.48	2.54	39.65	9.04	15.86	6.14	11.96	6.33
D	4.96	1.53	68.41	5.46	9.42	2.67	1.94	5.62
E	6.13	2.57	64.80	6.34	7.98	2.36	1.66	8.16
F	2.62	0.73	75.77	11.19	2.96	1.22	0.36	5.16

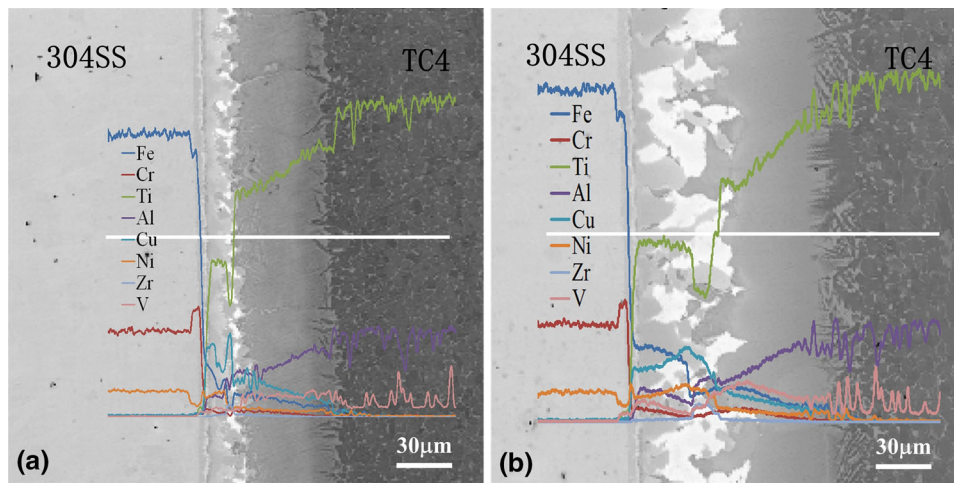


Fig. 6 Line scanning analysis results in the joints brazed with (a) $\text{Cu}_{43.75}\text{Ti}_{37.5}\text{Ni}_{6.25}\text{Zr}_{6.25}\text{V}_{6.25}$ (at.%) foil and (b) $\text{Cu}_{37.5}\text{Ti}_{25}\text{Ni}_{12.5}\text{Zr}_{12.5}\text{V}_{12.5}$ (at.%) foil

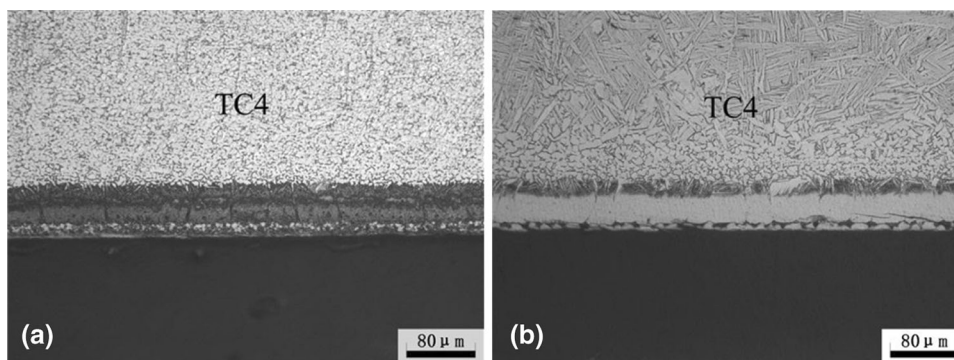


Fig. 7 Fracture location of the shear tested joints brazed with (a) $\text{Cu}_{43.75}\text{Ti}_{37.5}\text{Ni}_{6.25}\text{Zr}_{6.25}\text{V}_{6.25}$ (at.%) foil and (b) $\text{Cu}_{37.5}\text{Ti}_{25}\text{Ni}_{12.5}\text{Zr}_{12.5}\text{V}_{12.5}$ (at.%) foil

3. Results and Discussion

Figure 3 shows the microstructure of the TC4 titanium alloy/304 stainless steel (304SS) joints brazed with $\text{Cu}_{43.75}\text{Ti}_{37.5}\text{Ni}_{6.25}\text{Zr}_{6.25}\text{V}_{6.25}$ and $\text{Cu}_{37.5}\text{Ti}_{25}\text{Ni}_{12.5}\text{Zr}_{12.5}\text{V}_{12.5}$ (at.%) at 900 and 930 °C for 10 min, respectively. It can be seen that TC4 titanium alloy and 304 stainless steel substrates were tightly bonded through the filler metal. No pore and crack existed in the brazed seams. The thickness of the brazed seam was 80 μm with $\text{Cu}_{43.75}\text{Ti}_{37.5}\text{Ni}_{6.25}\text{Zr}_{6.25}\text{V}_{6.25}$ foil and 100 μm with $\text{Cu}_{37.5}\text{Ti}_{25}\text{Ni}_{12.5}\text{Zr}_{12.5}\text{V}_{12.5}$ foil. However, the thickness of the original filler metal was only 50 μm . This phenomenon suggests that diffusion and reaction occurred between the substrates and filler metal. It can be seen that the original boundary between the TC4 titanium alloy substrate and filler metal could not be discriminated in Fig. 3(b). Especially, the boundaries between the steel substrate and filler metal present fine serrated shape indicating partial dissolution of 304 stainless steel substrate.

It is worth noting that the microstructure of the TC4 titanium alloy substrate changed from fine equiaxed grain in the joint brazed with $\text{Cu}_{43.75}\text{Ti}_{37.5}\text{Ni}_{6.25}\text{Zr}_{6.25}\text{V}_{6.25}$ foil to lamellar structure in the joint brazed with $\text{Cu}_{37.5}\text{Ti}_{25}\text{Ni}_{12.5}\text{Zr}_{12.5}\text{V}_{12.5}$ foil, as shown in Fig. 3(a) and (b). Higher brazing temperature

for the joint brazed with $\text{Cu}_{37.5}\text{Ti}_{25}\text{Ni}_{12.5}\text{Zr}_{12.5}\text{V}_{12.5}$ foil led to this difference.

The backscattered electron images and EPMA map scanning results of the joints brazed with two foils are displayed in Fig. 4 and 5. It can be seen from Fig. 4(a) and 5(a) that a thin diffusion layer (marked as A) existed in the interface between the steel substrate and filler metal. And Fe from the steel substrate obviously diffused into the brazed seam, in Fig. 4(b) and 5(b). For the convenience of description, the gray, off-white, and light gray phases in the filler metal layer were marked with B, C, and D, respectively. E and F were marked in the reaction layers between TC4 titanium alloy substrate and filler metal.

The quantitative analysis results at A-F locations listed in Table 1 and 2 reveal that 11.24 and 14.26 at.% Fe were detected in location B. Location A, right in the interface between steel substrate and filler metal, contained 2.51-2.92 at.%Ti and 1.53-2.02 at.%V, indicating that Ti and V from the filler metal diffused into the steel substrate. It can be seen from Fig. 4(d) and 5(d) that Cr also diffused into the filler metal layer and even into the reaction layer between titanium substrate and filler metal. However, Cu and Ni mainly existed in the filler metal layer and slightly diffused towards two base metals. By comparing the quantitative results in locations A, E,

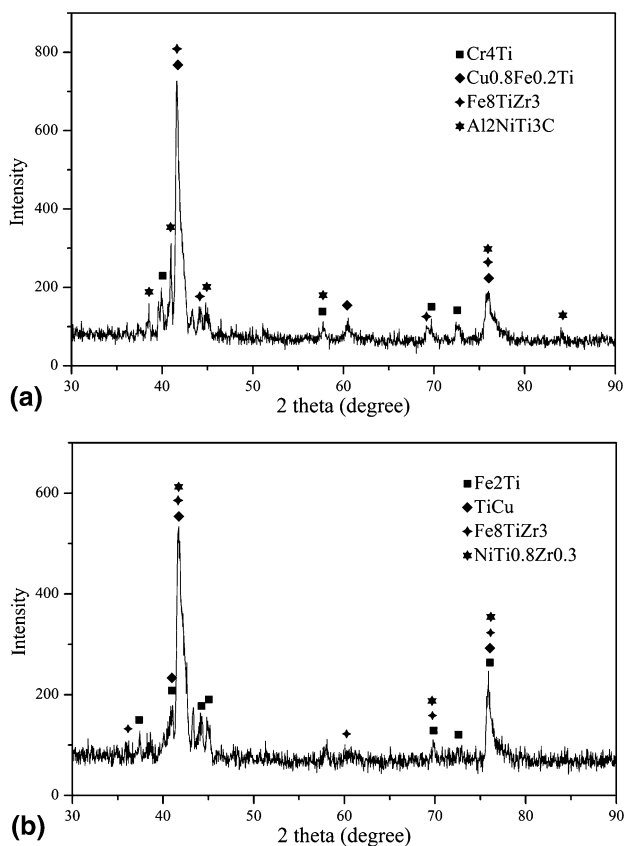


Fig. 8 XRD patterns of fractured joints brazed with (a) $\text{Cu}_{43.75}\text{Ti}_{37.5}\text{Ni}_{6.25}\text{Zr}_{6.25}\text{V}_{6.25}$ (at.%) foil and (b) $\text{Cu}_{37.5}\text{Ti}_{25}\text{Ni}_{12.5}\text{Zr}_{12.5}\text{V}_{12.5}$ (at.%) foil

and F in Table 1 and 2, Ni showed better affinity with steel substrate, but Cu displayed better affinity with titanium substrate. Zr almost existed only in the off-white region C; the measurements in Table 1 and 2 indicate that 11.07 and 11.96 at.% Zr were detected in location C which were far higher than in other locations.

Figure 6 shows the line scanning results in the joints brazed with $\text{Cu}_{43.75}\text{Ti}_{37.5}\text{Ni}_{6.25}\text{Zr}_{6.25}\text{V}_{6.25}$ and $\text{Cu}_{37.5}\text{Ti}_{25}\text{Ni}_{12.5}\text{Zr}_{12.5}\text{V}_{12.5}$ foils. It can be seen that the curve for Ti can be divided into five stages from right to left. They are successively flat stage in TC4 titanium alloy substrate, declining stage in the reaction layer between the titanium substrate and filler metal, valley stage in the off-white phase region, flat stage in the gray phase region in filler metal layer, and sharp drop stage in the interface between steel substrate and filler metal. It can also be clearly seen that the Fe and Ni contents dropped, but the Cr content raised, and a certain amount of Ti and V diffused into the 304SS substrate while observing the elemental curves in the interface between 304SS substrate and filler metal. The above phenomenon confirmed the quantitative analysis results in location A listed in Table 1 and 2, indicating good compatibility between 304 stainless steel and Cu-Ti-Ni-Zr-V filler metals. All alloying elements except Ti in the filler metal diffused into the reaction layer between TC4 titanium alloy substrate and filler metal, and their line scanning curves drop to the minimum in the interface between reaction layer and titanium substrate.

The joints brazed with $\text{Cu}_{43.75}\text{Ti}_{37.5}\text{Ni}_{6.25}\text{Zr}_{6.25}\text{V}_{6.25}$ and $\text{Cu}_{37.5}\text{Ti}_{25}\text{Ni}_{12.5}\text{Zr}_{12.5}\text{V}_{12.5}$ foils were shear tested at room

temperature. The results show that the shear strength of the joint brazed with $\text{Cu}_{43.75}\text{Ti}_{37.5}\text{Ni}_{6.25}\text{Zr}_{6.25}\text{V}_{6.25}$ foil was 105 MPa and that with $\text{Cu}_{37.5}\text{Ti}_{25}\text{Ni}_{12.5}\text{Zr}_{12.5}\text{V}_{12.5}$ foil was 116 MPa. However, the practical shear strength could be higher because two specimens brazed with $\text{Cu}_{43.75}\text{Ti}_{37.5}\text{Ni}_{6.25}\text{Zr}_{6.25}\text{V}_{6.25}$ foil and one specimen brazed with $\text{Cu}_{37.5}\text{Ti}_{25}\text{Ni}_{12.5}\text{Zr}_{12.5}\text{V}_{12.5}$ foil, during shear test, did not fail but the steel base metal bends over and the load was much higher than that for those specimens that broke through the brazed seam during shear test. Figure 7 shows the cross sections of the fractured joints on TC4 titanium side, and it can be clearly seen that the joints fractured through the gray phase (marked as location A in Fig. 4 and 5) in the filler metal layer. Figure 8 shows the XRD patterns of the fractured surfaces. Cr_4Ti , $\text{Cu}_0.8\text{Fe}_0.2\text{Ti}$, Fe_8TiZr_3 , and $\text{Al}_2\text{NiTi}_3\text{C}$ were found in the fractured joint brazed with $\text{Cu}_{43.75}\text{Ti}_{37.5}\text{Ni}_{6.25}\text{Zr}_{6.25}\text{V}_{6.25}$ foil, and Fe_2Ti , TiCu , Fe_8TiZr_3 and $\text{NiTi}_{0.8}\text{Zr}_{0.3}$ were detected in the joint brazed with $\text{Cu}_{37.5}\text{Ti}_{25}\text{Ni}_{12.5}\text{Zr}_{12.5}\text{V}_{12.5}$ foil. The existence of Cr-Ti, Fe-Ti, Cu-Fe-Ti, and Fe-Ti-V intermetallic compounds possibly caused the fracture of the resultant joints.

Because Ni can excellently solid solute with Fe in the steel substrate and Zr can completely solid solute with Ti in the titanium alloy base metal, and moreover, V has infinite solid solubility with both Fe and Ti; the fillers and two dissimilar base metals could mutually diffuse into each other to generate solid metallurgical bonding without forming massive harmful intermetallic compounds in the interfaces from the direct contact of Fe and Ti. Therefore, the developed Cu-Ti-Ni-Zr-V filler is supposed to be superior to Cu-Ti-Ni filler for joining TC4 titanium and type 304 stainless steel, due to the addition of Zr and V in the filler.

The fractographs of specimens are shown in Fig. 9, revealing brittle fracture features. The EDS analysis results in the marked locations are listed in Table 3. It can be seen that more than 26.66 at.% Fe was detected on both sides of the joint brazed with $\text{Cu}_{43.75}\text{Ti}_{37.5}\text{Ni}_{6.25}\text{Zr}_{6.25}\text{V}_{6.25}$ foil, especially in location 1; up to 49.40 at.% Fe and 15.79 at.% Cr were detected. It is significantly different from the results in other locations, indicating that the joint brazed with $\text{Cu}_{43.75}\text{Ti}_{37.5}\text{Ni}_{6.25}\text{Zr}_{6.25}\text{V}_{6.25}$ foil possibly fractured partially through the gray layer A. The results in locations 3, 4, and 5 in the joint brazed with $\text{Cu}_{37.5}\text{Ti}_{25}\text{Ni}_{12.5}\text{Zr}_{12.5}\text{V}_{12.5}$ foil listed in Table 3 were similar to the EPMA quantitative analysis results in gray layer (location B), as shown in Table 1 and 2. These results suggest that the fracture location of the joint brazed with $\text{Cu}_{43.75}\text{Ti}_{37.5}\text{Ni}_{6.25}\text{Zr}_{6.25}\text{V}_{6.25}$ foil is closer to the 304SS substrate, but the joint brazed with $\text{Cu}_{37.5}\text{Ti}_{25}\text{Ni}_{12.5}\text{Zr}_{12.5}\text{V}_{12.5}$ foil fractured through the gray layer (location B). However, the amount of the intermetallic phases identified might be very small because the detected layers were very thin, which explains the discrepancy between the XRD and EDS analysis results.

4. Conclusions

- (1) Vacuum brazing of TC4 titanium alloy and 304 stainless steel was conducted with newly developed $\text{Cu}_{43.75}\text{Ti}_{37.5}\text{Ni}_{6.25}\text{Zr}_{6.25}\text{V}_{6.25}$ and $\text{Cu}_{37.5}\text{Ti}_{25}\text{Ni}_{12.5}\text{Zr}_{12.5}\text{V}_{12.5}$ amorphous alloy foils, and solid joints without pore or crack in the brazed seam were obtained. The filler metal showed excellent compatibility with 304 stainless steel, and partial dissolution of 304 stainless steel substrate occurred during brazing.

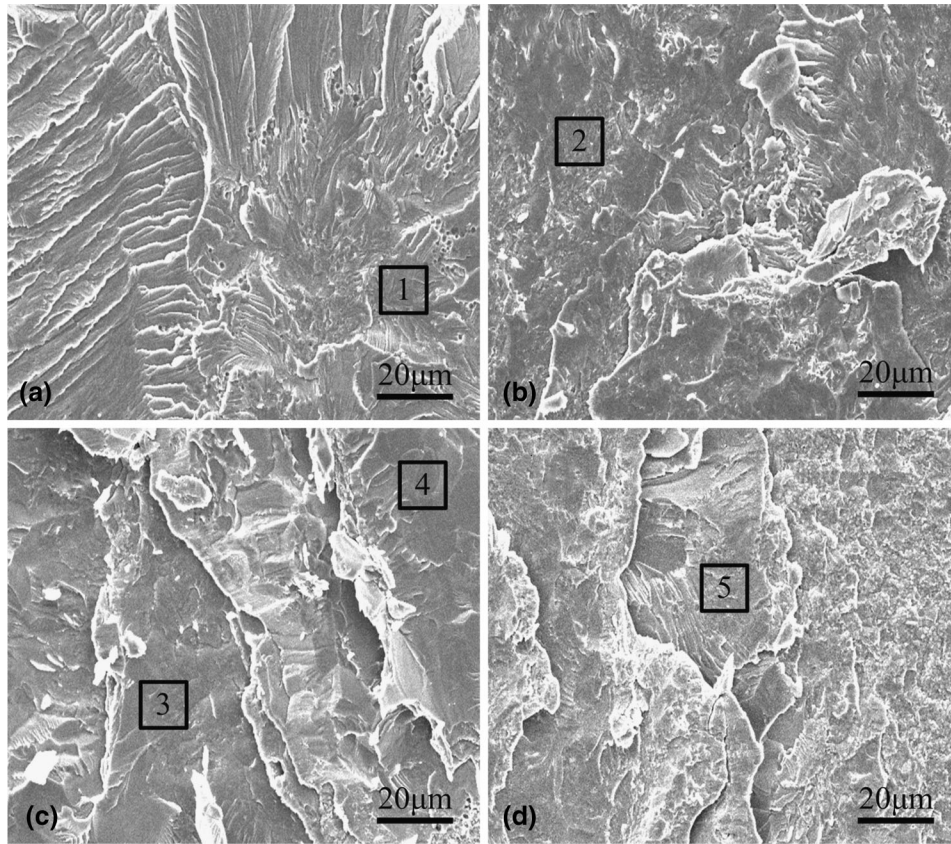


Fig. 9 Fractographs of joints brazed with (a, b) $\text{Cu}_{43.75}\text{Ti}_{37.5}\text{Ni}_{6.25}\text{Zr}_{6.25}\text{V}_{6.25}$ (at.%) foil and (c, d) $\text{Cu}_{37.5}\text{Ti}_{25}\text{Ni}_{12.5}\text{Zr}_{12.5}\text{V}_{12.5}$ (at.%) foil. Note: (a, c) on steel side and (b, d) on titanium side

Table 3 EDS analysis results in the locations marked in Fig. 9 (at.%)

Location	Fe	Cr	Ti	Al	Cu	Ni	Zr	V
1	49.40	15.79	27.63	1.50	0.95	2.97	1.50	0.25
2	26.66	3.76	54.39	2.98	4.52	3.97	1.98	1.74
3	15.99	2.96	50.48	8.85	10.04	5.38	2.89	3.40
4	12.09	1.41	60.99	3.52	6.68	6.07	5.62	3.61
5	16.03	2.38	55.42	3.00	11.01	6.17	1.41	4.57

(2) The shear strength of the joint brazed with $\text{Cu}_{43.75}\text{Ti}_{37.5}\text{Ni}_{6.25}\text{Zr}_{6.25}\text{V}_{6.25}$ foil was 105MPa and that with $\text{Cu}_{37.5}\text{Ti}_{25}\text{Ni}_{12.5}\text{Zr}_{12.5}\text{V}_{12.5}$ foil was 116 MPa. The joints fractured through the brazed seam with brittle fracture features.

(3) Cr_4Ti , $\text{Cu}_{0.8}\text{FeTi}$, Fe_8TiZr_3 , and $\text{Al}_2\text{NiTi}_3\text{C}$ phases were found in the fractured joint brazed with $\text{Cu}_{43.75}\text{Ti}_{37.5}\text{Ni}_{6.25}\text{Zr}_{6.25}\text{V}_{6.25}$ foil, and Fe_2Ti , TiCu , Fe_8TiZr_3 , and $\text{NiTi}_{0.8}\text{Zr}_{0.3}$ compounds were detected in that with $\text{Cu}_{37.5}\text{Ti}_{25}\text{Ni}_{12.5}\text{Zr}_{12.5}\text{V}_{12.5}$ foil. The existence of Cr-Ti, Fe-Ti, Cu-Fe-Ti, and Fe-Ti-V intermetallic compounds caused the fracture of the resultant joints.

Acknowledgments

This work was financially supported by the National Natural Science Foundation of China (Grant No. 51374048), the National Basic Research Program of China (973 Program, Grant No.

2011CB013402), the Fundamental Research Funds for the Central Universities, and the State Key Laboratory of Advanced Welding and Joining, Harbin Institute of Technology, Harbin, China.

References

1. R.R. Boyer, An Overview on the Use of Titanium in the Aerospace Industry, *Mater. Sci. Eng. A Struct.*, 1996, **213**(1–2), p 103–114
2. M. Yamada, An Overview on the Development of Titanium Alloys for Non-Aerospace Application in Japan, *Mater. Sci. Eng. A Struct.*, 1996, **213**(1–2), p 8–15
3. Z. Sun and R. Karppi, The Application of Electron Beam Welding for the Joining of Dissimilar Metals: An Overview, *J. Mater. Process. Technol.*, 1996, **59**(3), p 257–267
4. A. Fuji, T.H. North, K. Ameyama, and M. Futamata, Improving Tensile Strength and Bend Ductility of Titanium/AISI, 304L Stainless Steel Friction Welds, *Mater. Sci. Technol.*, 1992, **8**(3), p 219–235
5. W.B. Lee, Y.J. Kim, and S.B. Jung, Effects of Copper Insert Layer on the Properties of Friction Welded Joints Between TiAl and AISI, 4140 Structural Steel, *Intermetallics*, 2004, **12**(6), p 671–678

6. W.B. Lee, M.G. Kim, J.M. Koo, K.K. Kim, D. Quesnel, Y.J. Kim, and S.B. Jung, Friction Welding of TiAl and AISI4140, *J Mater Sci*, 2004, **39**(3), p 1125–1128
7. H.C. Dey, M. Ashfaq, A.K. Bhaduri, and K.P. Rao, Joining of Titanium to 304L Stainless Steel by Friction Welding, *J. Mater. Process. Technol.*, 2009, **209**(18–19), p 5862–5870
8. S. Meshram, T. Mohandas, and G. Reddy, Friction Welding of Dissimilar Pure Metals, *J. Mater. Process. Technol.*, 2007, **184**(1–3), p 330–337
9. N. Orhan, T.I. Khan, and M. Eroglu, Diffusion Bonding of a Microduplex Stainless Steel to Ti-6Al-4V, *Scripta Mater.*, 2001, **45**(4), p 441–446
10. S. Kundu, M. Ghosh, A. Laik, K. Bhanumurthy, G. Kale, and S. Chatterjee, Diffusion Bonding of Commercially Pure Titanium to 304 Stainless Steel Using Copper Interlayer, *Mater. Sci. Eng. A Struct.*, 2005, **407**(1–2), p 154–160
11. M. Ghosh, S. Kundu, S. Chatterjee, and B. Mishra, Influence of Interface Microstructure on the Strength of the Transition Joint between Ti-6Al-4V and Stainless Steel, *Metall. Mater. Trans. A*, 2005, **36A**(7), p 1891–1899
12. B. Kurt, N. Orhan, E. Evin, and A. Çalik, Diffusion Bonding between Ti-6Al-4V Alloy and Ferritic Stainless Steel, *Mater. Lett.*, 2007, **61**(8–9), p 1747–1750
13. S. Kundu, S. Sam, and S. Chatterjee, Interface Microstructure and Strength Properties of Ti-6Al-4V and Microduplex Stainless Steel Diffusion Bonded Joints, *Mater. Design*, 2011, **32**(5), p 2997–3003
14. S. Sam, S. Kundu, and S. Chatterjee, Diffusion Bonding of Titanium Alloy to Micro-Duplex Stainless Steel Using a Nickel Alloy Interlayer: Interface Microstructure and Strength Properties, *Mater. Design*, 2012, **40**, p 237–244
15. C.C. Liu, C.L. Ou, and R.K. Shiue, The Microstructural Observation and Wettability Study of Brazing Ti-6Al-4V and 304 Stainless Steel Using Three Braze Alloys, *J. Mater. Sci.*, 2002, **37**(11), p 2225–2235
16. R.K. Shiue, S.K. Wu, C.H. Chan, and C.S. Huang, Infrared Brazing of Ti-6Al-4V and 17-4 PH Stainless Steel with a Nickel Barrier Layer, *Metall. Mater. Trans. A*, 2006, **37A**(7), p 2207–2217
17. R.K. Shiue, S.K. Wu, and J.Y. Shiue, Infrared Brazing of Ti-6Al-4V and 17-4 PH Stainless Steel with (Ni)/Cr Barrier Layer(s), *Mater. Sci. Eng. A Struct.*, 2008, **488**(1–2), p 186–194
18. J.G. Lee, J.K. Lee, S.M. Hong, M.K. Lee, and C.K. Rhee, Microstructure and Bonding Strength of Titanium-to-Stainless Steel Joints Brazed Using a Zr-Ti-Ni-Cu-Be Amorphous Filler Alloy, *J. Mater. Sci.*, 2010, **45**(24), p 6837–6840
19. A. Elrefaey, L. Wojarski, J. Pfeiffer, and W. Tillmann, Preliminary Investigation on Ultrasonic-Assisted Brazing of Titanium and Titanium/Stainless Steel Joints, *Weld. J.*, 2013, **92**(5), p 148–153
20. R.K. Shiue, S.K. Wu, Y.T. Chen, and C.Y. Shiue, Infrared Brazing of Ti50Al50 and Ti-6Al-4V Using two Ti-based Filler Metals, *Intermetallics*, 2008, **16**(9), p 1083–1089
21. O. Botstein, A. Schwarzman, and A. Rabinkin, Induction Brazing of Ti-6Al-4V Alloy with Amorphous 25Ti-25Zr-50Cu Brazing Filler Metal, *Mater. Sci. Eng. A Struct.*, 1996, **206**(1), p 14–23
22. E. Ganjeh and H. Sarkhosh, Microstructural, Mechanical and Fractographical Study of Titanium-CP and Ti-6Al-4V Similar Brazing with Ti-based Filler, *Mater. Sci. Eng. A Struct.*, 2013, **559**, p 119–129
23. T. Noda, T. Shimizu, M. Okabe, and T. Iikubo, Joining of TiAl and Steels by Induction Brazing, *Mater. Sci. Eng. A Struct.*, 1997, **239–240**, p 613–618
24. H. Men, S. Pang, A. Inoue, and T. Zhang, New Ti-based Bulk Metallic Glasses with Significant Plasticity, *Mater. Trans.*, 2005, **46**(10), p 2218–2220
25. R. Messler, Jr., *Joining of Materials and Structures: From Pragmatic Process to Enabling Technology*, Butterworth-Heinemann, London, 2004